Myoelectric Control for Adaptable Biomechanical Energy Harvesting

Jessica C. Selinger and J. Maxwell Donelan

***Abstract*—We have designed and tested a myoelectric controller that automatically adapts energy harvesting from the motion of leg joints to match the power available in different walking conditions. To assist muscles in performing negative mechanical work, the controller engages power generation only when estimated joint mechanical power is negative. When engaged, the controller scales its resistive torque in proportion to estimated joint torque, thereby automatically scaling electrical power generation in proportion to the available mechanical power. To produce real-time estimates of joint torque and mechanical power, the controller leverages a simple model that predicts these variables from measured muscle activity and joint angular velocity. We first tested the model using available literature data for a range of walking speeds and found that estimates of knee joint torque and power well match the corresponding literature profiles (torque R^2: 0.73–0.92; power R^2: 0.60–0.94). We then used human subject experiments to test the performance of the entire controller. Over a range of steady state walking speeds and inclines, as well as a number of non-steady state walking conditions, the myoelectric controller accurately identified when the knee generated negative mechanical power, and automatically adjusted the magnitude of electrical power generation.**

***Index Terms*—Energy harvesting, exoskeletons, gait, myoelectric control, terrain adaptation.**

I. Introduction

THIS decade has seen rapid progress in the development of powered exoskeletons designed to augment the function of human joints [1]–[3]. Within this larger field of wearable robotics, our focus has been on developing devices to capture mechanical energy normally lost to heat during walking and convert it to electricity [4], [5]. Although these biomechanical energy harvesters are exoskeletons, we have not designed them to provide additional torque whenever the user needs it. Instead, our design goal is to generate useful amounts of electrical energy without substantial increases in user effort. To do so, we control the timing and magnitude of power generation such that it assists muscles in performing negative mechanical work [4], [5]. Although the intended use is different than most powered exoskeletons, the control goal is similar—to apply torque with the ideal timing, direction and magnitude.

Manuscript received May 21, 2015; revised November 19, 2015; accepted December 08, 2015. Date of publication December 22, 2015; date of current version March 04, 2016. The work of J. C. Selinger was supported by the Vanier Canadian Graduate Scholarship. The work of J. M. Donelan was supported by the U.S. Army Research under Grant W911NF-13-1-0268.

The authors are with the Department of Biomedical Physiology and Kinesiology, Burnaby, BC, V5A 1S6 Canada (e-mail: jessica_selinger@sfu.ca; mdonelan@sfu.ca).

Color versions of one or more of the figures in this paper are available online at http://ieeexplore.ieee.org.

Digital Object Identifier 10.1109/TNSRE.2015.2510546

A central challenge of effective exoskeleton design is a controller that automatically adapts its action to match the requirements of different phases of the gait cycle and different walking conditions. For example, it may be desirable for a powered exoskeleton to assist trailing leg push-off work during walking [6]–[10]. The timing and magnitude of helpful push-off work will likely depend on both walking speed and slope [6], [11], [12]. Energy harvesting from leg joint motion faces similar challenges—the negative joint work available for harvesting, as well as the magnitude of torque required to do so effectively, depend on the phase of the walking cycle [13], [14]. For example, the knee joint generates negative mechanical work with large extension torques at slow flexion speeds at the beginning of stance, and with small flexor torques at high extension speeds at the end of swing [15], [16]. An ideal energy harvester controller would adapt its resistive torque to match that available from the knee at each phase of the walking cycle [14], [17]. Furthermore, as walking speed changes, the appropriate level of torque for each phase also changes. And at different walking slopes, some phases of the walking cycle may stop producing negative work whereas others might start [18], [19]. More generally, a typical walking bout in the real world does not occur at a steady state speed or slope. Instead, it involves speeding up and slowing down while walking over variable terrain and negotiating disturbances such as stepping over obstacles. An ideal exoskeleton controller would adapt its action to optimize its performance under these variable conditions.

To effectively adapt the action of an exoskeleton, a controller needs to measure or estimate the required joint torque. One logical method is to measure the electrical activity of the muscles that are typically responsible for the joint torque. These electromyography (EMG) signals, which can be noninvasively measured from the surface of the skin, indicate the activation of the underlying muscle and give indirect insight into its force [20]–[22]. Conveniently, EMG also provides advanced insight into user intent as the measured activity precedes force generation by approximately 20–100 ms [23], [24]. As a consequence of these benefits, EMG has been used extensively to control upper limb prosthetics [25]–[27] and is beginning to be employed in the control of lower limb prosthetics [28], [29]. Ferris and colleagues are among the first to develop myoelectric controllers for lower limb exoskeletons [30], [31]. In their ankle-foot orthoses, the air pressures of two artificial pneumatic muscles—a plantar flexor and a dorsi flexor—are regulated in proportion to the activity of the soleus and tibialis anterior muscles. Naïve users are able to quickly adapt to walking with the novel device by adjusting muscle activity to take advantage

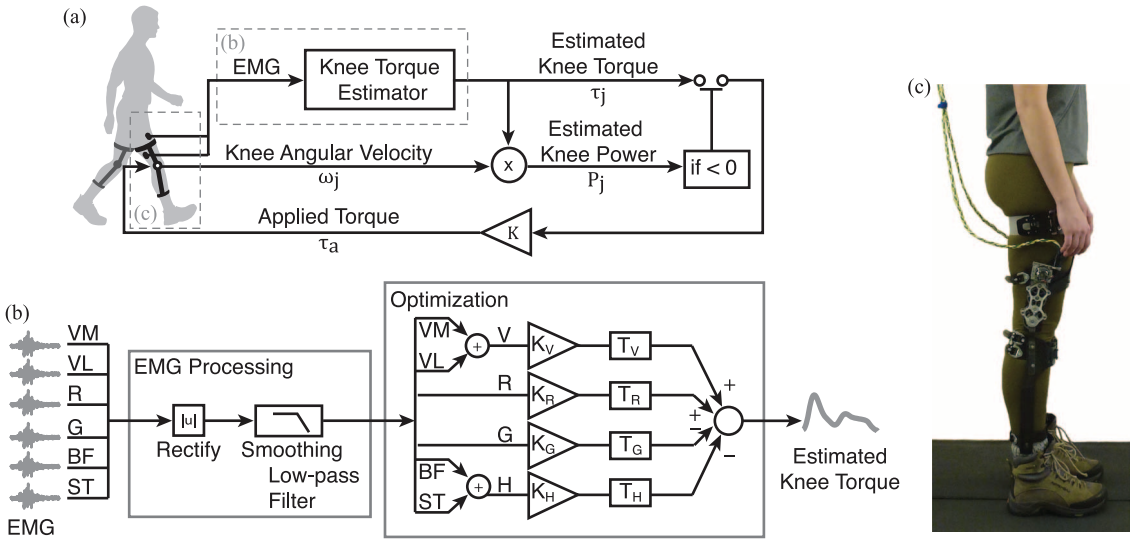

Fig. 1. Myoelectric control system for an energy harvesting exoskeleton. (a) Controller design. Muscle activity is used to produce a real-time estimate of knee joint torque. The product of this estimate and knee angular velocity produces an estimate of knee joint power. A resistance proportional to knee joint torque (by a factor K) is applied only during negative work phases of gait, when knee joint power is negative. (b) Torque estimation. Raw EMG signals from the vastus medialis (VM), vastus lateralis (VL), rectus femoris (R), medial gastrocnemius (G), biceps femoris (BF) and semitendinosus (ST) are rectified and smoothed. The VM and VL are summed, as are the BF and ST, resulting in four muscle activity profiles. A constrained nonlinear optimization is then used to identify four optimal gains (K_V, K_R, K_G and K_H) and delays (T_V, T_R, T_G and T_H), and the resulting four profiles are summed to produce an estimate of knee joint torque. (c) Exoskeleton hardware. The custom carbon fiber shell is mounted to the thigh and shank using nylon and polyethylene strapping. The steal gear train transmits rotation at the knee joint to the rotor of a magnetic motor. EMG electrodes, placed on the quadriceps and hamstring muscles, are used to measure muscle activity, which is in turn used to control harvesting. While the exoskeleton is identical to that used in the experiment, the picture is of a different subject.

of the exoskeleton assistance [30]. The Hybrid Assistive Leg (HAL-5) exoskeleton developed by the University of Tsukuba, Japan also uses myoelectric signals as inputs into their controller. But, rather than simply make actuator activity proportional to a single muscle's EMG, this controller uses the measured activity to first estimate joint torque, which is in turn used to control the exoskeleton torque [32]. Although most lower limb exoskeletons rely on other methods to control their action [3], the success of the few existing devices that employ myoelectric control, as well as the promise of tapping into the user's own intentions, highlight the potential of myoelectric controllers.

Our purpose in this study was to design a myoelectric controller that would automatically adapt energy harvesting to match the mechanical power available in different walking conditions, and then test its performance. As detailed in the next section of this paper, our controller uses real-time estimates of joint torque and mechanical power to determine the timing and magnitude of electrical power generation. The following section describes our model for estimating joint torque and mechanical power from measured muscle activity and joint angular velocity. It includes a relatively simple procedure for identifying the unknown model gains and delays, and then tests the model performance against literature data collected at a range of walking speeds. In the final section, we combine our candidate controller and our model for estimating joint torque and power to control energy harvesting exoskeletons worn by a human subject. We test its ability to automatically adapt the timing and magnitude of electrical power generation across a range of steady state walking speeds and slopes, as well as a number of non-steady state walking conditions.

II. Controller Design

Our controller relies on real-time estimates of knee joint torque (τ_j) and knee joint angular velocity (ω_j), the product of which produces an estimate of knee joint power (P_j) [Fig. 1(a)]. We designed our controller to engage power generation only when estimated knee joint power is negative. When engaged, the resistive torque that the exoskeleton applies to the body (τ_a) is made proportional to knee joint torque by a constant K

$$\tau_a = \begin{cases} K \cdot \tau_j, & \text{if } P_j < 0 \\ 0, & \text{otherwise} \end{cases}. \quad (1)$$

Since the total torque acting about the knee joint (τ_j) is the sum of the torque provided by the body (τ_j) and the exoskeleton (τ_a), the fraction of total torque contributed by the exoskeleton can be expressed as

$$\frac{\tau_a}{\tau_t} = \frac{K}{K+1}. \quad (2)$$

If $K = 1$, the exoskeleton and joint each contribute half of the total torque. If K is reduced to 0.5, the torque fraction applied by the exoskeleton would drop to 1/3 with the remainder contributed by the body. This relationship, between the torque applied by the body and that by the exoskeleton, is also true of the mechanical power generated by the body and exoskeleton. This is because the joint and exoskeleton share a common angular velocity at the point of torque application. When the exoskeleton generates negative mechanical power on the body, the body generates positive mechanical power on the exoskeleton. This positive mechanical power is converted into electrical power with an efficiency determined by the exoskeleton components including

its transmission, generator and power conditioning circuitry [5]. Thus, our controller automatically scales electrical power generation to be proportional to the available negative mechanical power at the joint, with the proportion determined by K.

It is not possible to predict an optimal value of K without human experiments. Very low values of K are undesirable because the resulting low applied torque would leave some available negative mechanical work untapped for power generation. It is likely that very high values of K are also undesirable because a user's nervous system may not be able to adapt its control of muscle forces to take advantage of the assistance provided by the exoskeleton. This would result in a greater than required total torque at the knee, leading to a stiff-kneed gait with very little knee motion and thus very little mechanical power available for harvesting. If users are able to dramatically reduce the torque generated by their muscle, high values of K may still not be desirable because the resulting low EMG signals may become insufficient for control. Finally, it is likely that users will be more perturbed by the inevitable errors in estimated torque, especially timing errors, when the exoskeleton attempts to apply the large torques associated with high values of K. The ideal value for K lies somewhere between the two extremes, and can be determined using human experiments to compare power generation, comfort, and muscle activity at different values of K.

Overall, our simple controller structure is inherently adaptable to varying gaits and movements, as it does not rely on prior knowledge of standard knee joint kinematics or kinetics. Indeed, if knee joint torque and angular velocity are accurately estimated, the controller should engage and disengage power generation appropriately, regardless of the task. While we have chosen to estimate knee joint torque from muscle activity, and knee angular velocity from generator voltage (discussed below), our controller is not specific to these measures, or even to the knee joint; it could use other means to estimate joint torque and angular velocity in real-time, and can be applied to other biological joints.

III. Joint Torque and Power Model

Our model estimates knee joint torque and mechanical power using measured muscle activity and joint angular velocity. To design our model, we have used literature data, including knee joint angular velocity, torque and power [15], as well as lower limb muscle activity [33]. As detailed below, we first identify unknown model parameters, including gains and delays, using knee joint flexor and extensor muscle activity during level walking at a moderate speed. We then tested our model's robustness to predicting knee joint dynamics across a range of magnitudes and timings by comparing our estimated knee joint torque and power to literature values across a range of walking speeds.

A. Model Designs

Our model incorporates muscle activity from three knee extensors—vastusmedialis (VM), vastuslateralis (VL), and rectus femoris (R)—as well as from three knee flexors—biceps femoris (BF), semitendinosus (ST), medial gastrocnemius (G) [Fig. 1(b)]. The activity of these muscles can be easily measured using surface EMG. In the design of our model, we used average rectified and smoothed muscle activity profiles from the literature that were collected during level walking at 1.25 m/s [33]. These signals were further smoothed using a critically damped 6 Hz low pass filter. Next, activity from VM and VL, which are of similar profile shape, were summed to create one vastus muscle activity profile (V). The BF and ST were also summed, creating a single hamstring muscle activity profile (H). No normalization or weightings were applied to the signals prior to summing. Using the resulting four muscle activity profiles (V, R, H, and G) we sought to produce an estimate of joint torque, which, when multiplied by angular velocity, would produce an estimate of joint power.

B. Parameter Identification

We used constrained nonlinear optimization to solve for four gains (K_V, K_R, K_H, and K_G) and four time delays (T_V, T_R, T_H, and T_G) that we applied to the V, R, H, and G profiles prior to summing these signals to produce an estimate of joint torque. These parameters were optimized such that the resulting estimate of joint torque, when multiplied by knee angular velocity, produced an estimate of joint power that best fit the literature knee joint mechanical power for the same walking speed [15]. That is, the root mean square error was between the estimated and literature joint power was minimized. While it is also possible to optimize these parameters such that they produce the best-fit estimate of knee joint torque, we have chosen to optimize for power because our intended application is energy harvesting during phases of negative mechanical joint power. By optimizing for power we are in effect optimizing for torque that is weighted by angular velocity, with phases of high angular velocity assigned greater importance than those with low angular velocity. For other applications, such as powered exoskeletons, it may be more useful to simply optimize for torque. The optimization was implemented using Matlab's fmincon function (Mathworks, NA, USA). The constraints applied to the optimization required positive magnitudes for the knee extensor gains (K_V and K_R) and negative magnitudes for the knee flexor gains (K_H and K_G). Additionally, we restricted the magnitudes of the four time delays to lie within 0–100 ms, which encompasses reasonable predictions of electromechanical delay in working muscle [23], [24].

Using this model and our optimized parameters, we were able to produce EMG-derived estimates of knee joint torque and power that well matched literature profiles collected at the same walking speed (torque R^2: 0.92, power R^2: 0.94, Fig. 2, Table I). As expected, the vastus muscle profile (V) contributed most substantially to the large net knee extensor torque during mid stance, while the hamstring profile (H) accounted for the net flexor torque during late swing to early stance. The rectus femoris (R) and medial gastrocnemius (G) activity profiles made substantially smaller contributions, but did improve the optimized fit to the more subtle net extensor and flexor torque evident at mid gait cycle. The literature knee joint power data that we used to identify model parameters were collected on different subjects, and by different authors, than the measures of muscle activity. This provides an initial indication that we

TABLE I
OPTIMIZED MODEL PARAMETERS AND RESULTING TORQUE AND POWER R^2 VALUES FOR LITERATURE AND EXPERIMENTAL DATA

	Time Delay (ms)				Gain (Nm/μV)				R^2	
	T_V	T_R	T_G	T_H	K_V	K_R	K_G	K_H	Torque	Power
Literature: Right	83	0	7	83	0.42	0.14	-0.72	-0.33	0.92	0.94
Experimental: Right	38	0	0	31	1.09	0.00	-0.34	-0.39	0.92	0.79
Experimental: Left	19	67	0	23	0.98	0.32	-0.26	-0.39	0.92	0.81

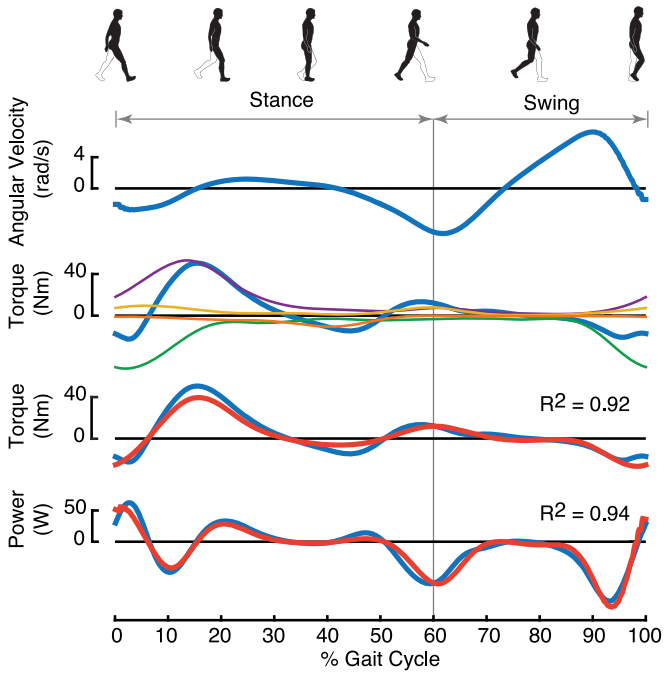

Fig. 2. Parameter estimation using literature EMG. Literature knee joint angular velocity, torque and mechanical power (blue; all plots) [15]. Literature EMG signals [33] were used to identify optimal model parameters, including four gains and four delays, which when applied to muscle activity profiles produced the V, R, G, and H traces (purple, yellow, orange, and green, respectively; second plot). Summing these traces produces the torque estimate (red; third plot), while taking the product of angular velocity and the torque estimate produces the power estimate (red; fourth plot). All literature data were from level walking at 1.25 m/s.

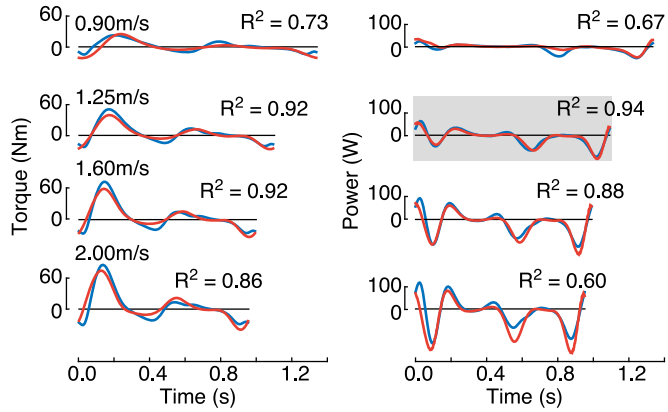

Fig. 3. Parameter validation for a range of walking speeds using literature EMG. EMG profiles from the literature [33] were used to derive estimates of knee torque (red; left column) and power (red; right column) that were compared to literature knee joint torque (blue; left column) and mechanical power (blue; right column) for various walking speeds (0.90, 1.25, 1.60, and 2.00 m/s) [15]. Although model parameters were optimized only for power at 1.25 m/s (grey shading), these same parameters well predicted knee joint torque and power across a wide range in walking speed. The x-axes are expressed in time, as opposed to percent-normalized gait cycle, allowing better visualization of the absolute changes in timing for the various gait speeds presented.

may not need subject-specific measures of joint power when identifying model parameters for individual users.

C. Parameter Validation

We next assessed if our optimized gains and delays could be used to produce accurate EMG-derived estimates of knee joint torque and power across a range of walking speeds. It is important for us that the solved parameter values generalize to walking conditions beyond which they were optimized for, as this allows us to use a relatively simple and short procedure for identifying model parameters. We used the gains and time delays identified at a walking speed of 1.25 m/s to estimate torque and power profiles for speeds ranging from 0.9 m/s to 2.0 m/s. We used varying speeds to test our model's generalizability because changes in speed result in changes in both the timing and magnitude of joint torque and power. While EMG and kinetic data are readily available in the literature across a range of speeds, exact speed matches were not. Here, we used EMG data from Hof and colleagues, collected at speeds of 0.75, 1.00, 1.25, 1.50, and 1.75 m/s, and kinematic and kinetic data from Zelik and Kuo, collected at speeds of 0.70, 0.90, 1.25, 1.60, 1.80 m/s [15], [33].

We found that we could generate reasonably accurate estimates of torque and power for a range of walking speeds using parameters optimized at a single comfortable walking pace (Fig. 3). Although torque and power estimates did worsen as speeds differed from 1.25 m/s, the R^2 of our estimates remained above 0.70 for torque and 0.60 for power at all speeds. The magnitudes of the torque and power estimates were appropriately scaled across the range of speeds. Moreover, the timing of negative and positive torque and power phases were quite accurate despite large changes in stride times across different speeds. Overall, our findings indicate that using a relatively small number of muscles and a simple procedure for optimizing model parameters, it is possible to predict knee joint torque and power across a range of locomotor patterns.

D. Alternative Models

We tested a number of alternative models for estimating knee joint torque and power that leveraged different combinations of muscles. For example, we tried including only uni-articular knee extensors (VM and VL) and flexors (BF and ST). However, it was clear that, for level walking at 1.25 m/s, our poorest estimates of torque occurred during the end of stance and beginning of swing (30%–70% gait cycle) and, as a result, we largely missed the substantial phase of negative joint power that peaks at around 60% of the gait cycle. This is not surprising, as the uni-articular knee extensors and flexors are nearly inactive

during this portion of the gait cycle. The addition of G and R, which demonstrate peak activity in this otherwise silent phase, allowed for better fitting of these subtle mid gait cycle flexor and extensor peaks in torque. Overall, models that do not include G and R are still able to account for about 85% of the variation in torque and power, but their inclusion improves this to over 90%. A limitation of including bi-articular muscles in our model is that muscle activity will be interpreted as acting at the knee, whereas the primary purpose may be to act at other joints, such as the ankle or hip.

Our model estimates of torque and power are less impacted by the removal of other, more redundant, muscles. Muscle activities from the two vasti are quite similar. Therefore, it is possible to remove either the VL or VM and still explain over 90% of the variation in torque and power. The same is true for the two hamstrings; either the BF or ST can be removed. We have chosen to sum the activity from VM and VL, as well as that from BF and ST, because, for our purposes, it was easy to instrument both. However, in situations where hardware or accessibility to muscle electrode sites is limited, it appears that our model could function equally well with EMG recordings from only four non-redundant muscles per leg.

IV. Experimental Testing

Here we preformed preliminary experiments to test the ability of our controller, and the joint torque and power model that it relies on, to control energy harvesting exoskeletons worn by a human subject. Our primary aim was to assess if our myoelectric controller could be used to accurately identify when the knee is generating negative mechanical power, and automatically adjust the magnitude of electrical power generation to match the available mechanical power.

Performing human experiments allowed us to test our controller in ways not possible using only available literature data. For one, we assessed if our simple parameter estimation procedure sufficiently predicted knee joint toque and power profiles when relying on EMG data from a single subject, as opposed to data averaged over multiple subjects. We were also able to test if, when the controller is turned on, our estimates of knee joint torque and power were still reliable, despite the potentially perturbing effects of the exoskeleton resistance. We were also able to explore what fraction of total knee joint torque, defined by K, was optimal for the user—a question we are unable to assess without instrumenting a human with the exoskeleton. Lastly, when attempting to validate our solved controller parameters, we were able to asses not only changes in torque timing and magnitude across steady state walking speeds, for which literature EMG data were available, but also across different inclines and in a number of non-steady state walking conditions.

A. Hardware

We used wearable energy harvesting exoskeletons that couple knee joint movement to generator rotation, allowing us to convert mechanical to electrical power. These novel exoskeletons differ from those on which we have previously reported [4], [13]—they perform bi-directional energy harvesting, generating electrical power during both knee joint flexion and extension. Each exoskeleton weighs 1.1 kg and is comprised of a custom carbon fiber shell and custom steel gear train coupled to an off-the-shelf rotary magnetic generator (BLDC40S-10A, NMB Technologies Inc.) [Fig. 1(c)]. During walking, the relatively low angular velocity and high torque characteristics of knee motion are transformed by the gear train to produce relatively high angular velocity and low torque at the generator. This rotational motion in the generator's rotor induces voltage in the windings and, if the controller allows it, electrical current in the windings [13]. The induced current generates its own magnetic field that resists the motion of the knee with a torque proportional to the current magnitude. We limited the maximum torque to 11 Nm based on the designed strength of the gear train. We estimated the torque applied to the knee from the product of the measured generator current, the generator's torque constant ($3.36 \times$ 10-2 Nm/A) and the exoskeleton gear ratio (110:1). We also estimated the magnitude of knee angular velocity from the product of measured generator voltage and the generator's velocity constant (0.33 Rad/s/V). We determined the direction of generator rotation from the voltage phase relationship between the generator's three phases.

B. Subject Instrumentation

We performed testing on a single able-bodied subject (body mass: 88 kg; height: 180 cm) during a single 6-h testing session. Simon Fraser University's Office of Research Ethics approved the protocol, and the participant gave their written, informed consent before experimentation. We placed EMG electrodes bilaterally on the subject's knee joint extensors (VM, R, VL) and flexors (BF, ST, and G) (Bagnoli Desktop EMG, Delsys Inc., MA, USA). EMG signals were full wave rectified and smoothed using a 3 Hz low pass filter. The subject donned an exoskeleton on each leg. All walking was carried out on an instrumented treadmill (FIT, Bertec Inc., OH, USA). We used custom software to measure muscle activity, generator voltages and generator currents in real-time. This same software used our model to calculate desired exoskeleton torque based on measured EMG, and desired generator current based on desired torque. The software commanded the desired current to a custom current control unit, which performed high-frequency closed-loop control of the current drawn from each exoskeleton to match the desired current, and thus match the actual torque to the desired torque. We implemented the real-time software using Simulink and Real-Time Windows Target (Mathworks, NA, USA). All signals were sampled and commanded at 1000 Hz (NI DAQ PC1-6071E, National Instruments Corporation, TX, USA).

C. Parameter Identification

To identify optimal model parameters for our test subject, they first walked on the level treadmill at 1.5 m/s for 6 min while wearing the exoskeleton with the controller turned off. EMG signals (Fig. 4) from the last 3 min were then used to solve for the optimal muscle gains (K_V, K_R, K_H, and K_G) and time delays (T_V, T_R, T_H, and T_G) for each leg that best fit literature knee power profiles [15] for a similar walking speed (1.6 m/s).

Using these optimized parameters, we were again able to produce accurate estimates of both knee torque and power (Fig. 5, Table I). Our estimates of knee joint torque using EMG from our single test subject matched the literature knee joint torque

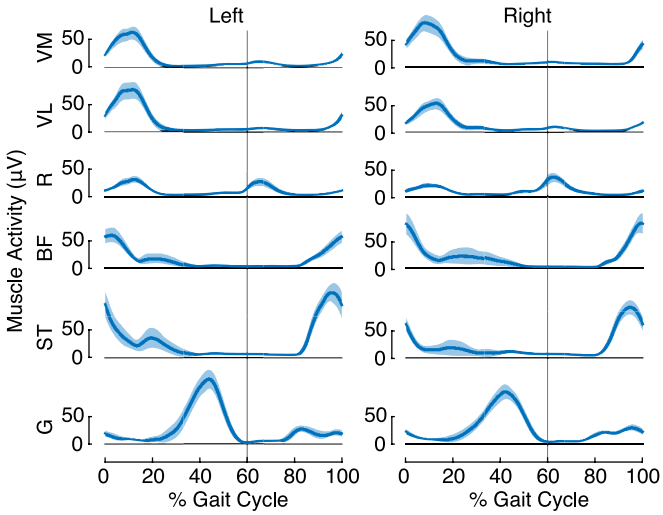

Fig. 4. EMG for the right and left leg collected during level walking at 1.5 m/s. Muscles include the vastus medialis (VM), vastus lateralis (VL), rectus femoris (R), biceps femoris (BF) and semitendinosus (ST) and medial gastrocnemius (G). Shaded regions represent ±1 SD.

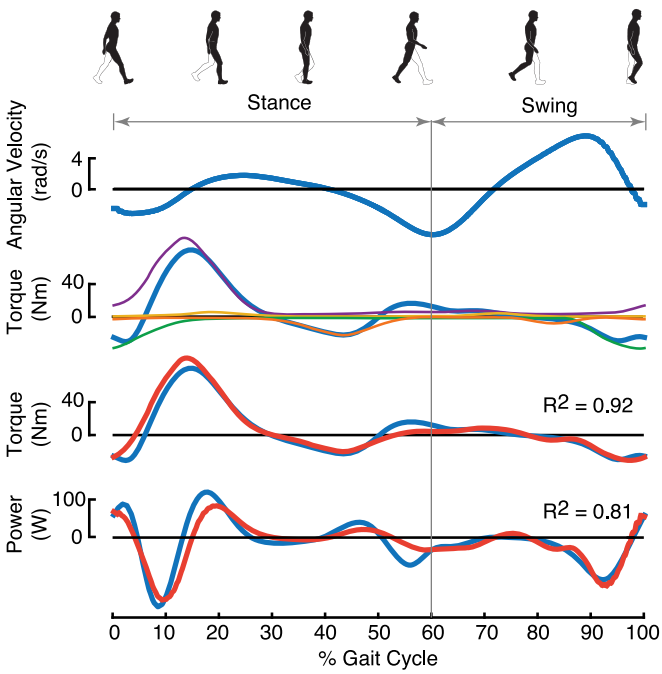

Fig. 5. Parameter estimation using experimental EMG. Literature knee joint angular velocity, torque and mechanical power (blue; all plots) [15]. Measured EMG signals [33] were used to identify optimal model parameters, including four gains and four delays, which when applied to muscle activity profiles produced the V, R, G, and H traces (purple, yellow, orange, and green, respectively; second plot). Summing these traces produces the torque estimate (red; third plot), while taking the product of angular velocity and the torque estimate produces the power estimate (red; fourth plot). All EMG data were measured during level walking at 1.5 m/s. Data presented is from the left leg.

just as well as the estimate derived from literature EMG, which was averaged across multiple subjects (R^2: 0.92 for both literature and experimental data). Our experimental estimates of joint power were somewhat worse, but still explained approximately 80% of the variability in literature mechanical knee joint power.

A comparison of the optimized parameters from the left and right legs showed many similarities (Table I). The knee flexors,

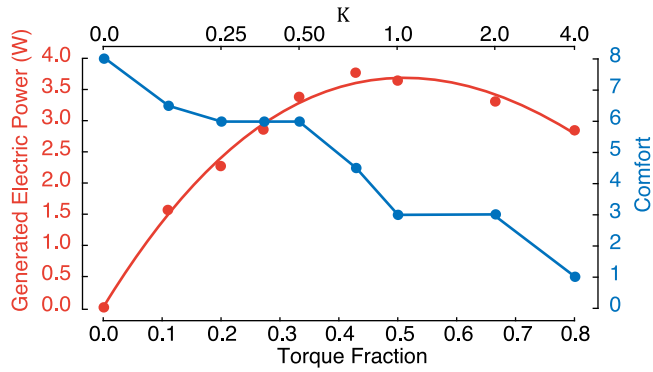

Fig. 6. Generated electric power (red) and comfort scores (blue) across a range of torque fractions applied by the exoskeleton. The proportionality constant (K) determines the fraction of the total knee joint toque applied by the exoskeleton [Eq. (2), Torque Fraction]. Electric power data presented is from the left leg.

including H and G profiles, were similarly weighted for the two legs and exhibited comparable time delays. The same was true for the dominant extensor profile, V. However, for the right leg the extensor R profile was assigned a zero weighting, while for the left a non-zero gain was found to be optimal. A sensitivity analysis on our optimized gains revealed that the R profile for the left leg could have also been removed, by setting the gain to zero, and R^2 values would be minimally affected ($\Delta R^2 < 0.01$). This is largely because the VM and VL for our experimental subject were active during mid gait cycle, unlike in the literature data. It is possible that the measured activity was truly emanating from the vasti, or that we picked up cross talk from RF. In either case, it made collection from RF redundant for our particular subject. Although the RF muscle could have been removed for both legs, we chose to proceed with the identified optimal gains.

D. Optimal Torque Fraction

Here we identify an optimal fraction of total knee joint torque to be applied by the exoskeleton [eq. (2)]. Our optimized gains and time delays are used to estimate joint torque and power, and the exoskeleton only applies a resistive torque, proportional to joint torque, when joint power is negative. We use a proportionality constant (K) between estimated and applied torque to tune this fraction [eq. (2)].

To determine the optimal torque fraction applied by the exoskeleton, we had the subject walk at a range of values for K (0, 0.125, 0.25, 0.375, 0.5, 0.75, 1, 2, and 4) that spanned torque fractions from 0 to 4/5. Order was randomized. They walked at each K for 3 min at 1.5 m/s on the level treadmill, and data from the last 1 min was used for analysis. For each K, the subject also verbally rated their level comfort on a scale of 1 to 10 (10 being the most comfortable and 1 being the least).

We found a parabolic relationship between harvested power and torque fraction applied by the exoskeleton (Fig. 6). Harvested power appeared to peak at a K of around 1, which corresponds to a torque fraction of 1/2. However, because comfort scores dropped between a K of 0.5 and 1 (from a score of 6 to 3), we selected a K of 0.5 for all subsequent testing. Muscle activity of the knee flexors and extensors showed trends consistent with these subjective comfort scores, where EMG activity steadily

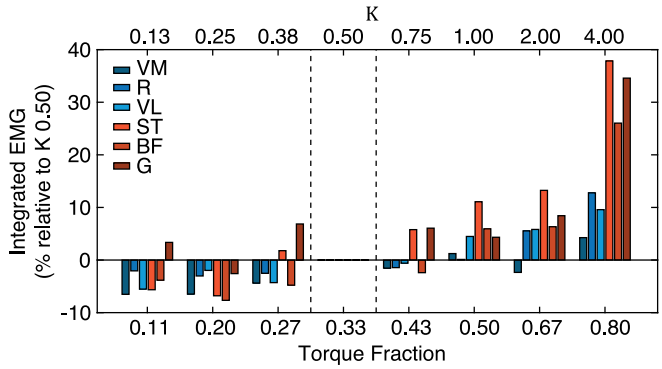

Fig. 7. Integrated EMG throughout the gait cycle for the knee extensors (blue shades) and flexors (red shades) for a range of torque fractions applied by the exoskeleton. Muscle activity is normalized to activity from the chosen torque fraction of 1/3 ($\mathrm{K} = 0.50$).

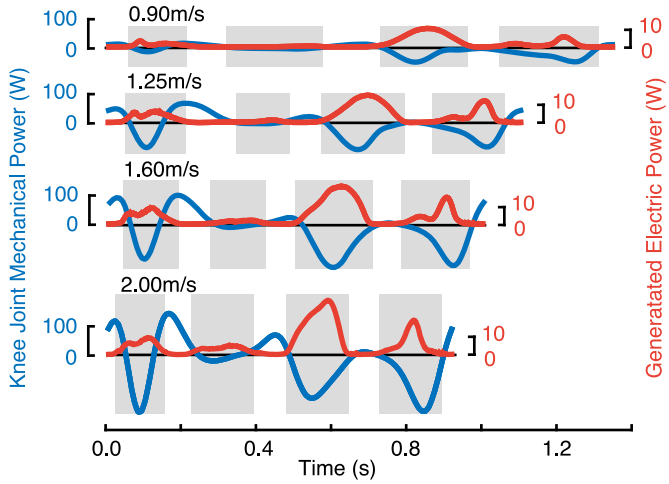

Fig. 8. Generated electric power (red) compared to literature knee joint mechanical power (blue) for various walking speeds. Shaded regions represent phases of the gait cycle during with the exoskeletons engaged power generation. Data presented are from the left leg.

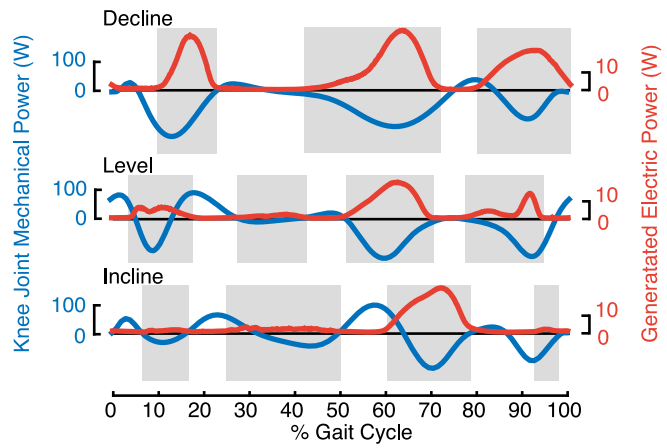

Fig. 9. Generated electric power (red) is compared to literature knee joint torque and mechanical power (blue) for decline ($-15°$), level ($0°$) and incline ($+15°$) walking at 1.5 m/s. Shaded regions represent phases of the gait cycle during with the exoskeletons engaged power generation. Data presented are from the left leg.

increased for gains above 0.50 (Fig. 7). This chosen gain corresponds to a torque fraction of 1/3, and harvested power was still 90% of the maximal produced at a gain of 1.

E. Parameter Validation

We next assessed if our optimized model parameters and K could be used to control energy harvesting for a human walking at different steady state and non-steady state gaits. To be useful in real-world walking conditions, our controller must be adaptable to various self-selected gaits, such as different walking speeds, as well as imposed changes in gait, such as those adopted when one encounters a sloped terrain. Moreover, our controller would ideally be adaptable to sudden single step changes in gait, such those taken when stepping over an object or down from an object. We sought to determine if our controller could accurately identify when the knee is generating negative mechanical power, and then automatically adjust the magnitude of electrical power generation for these range of conditions.

To produce different steady state gait patterns that varied the timing and magnitude of negative mechanical knee joint power, we had the subject walk at a range of speeds and slopes. They walked for 2 min at speeds of 0.9, 1.25, 1.6, and 2 m/s on the level treadmill, in randomized order. They also walked for 2 min at slopes of $-15°$, $0°$, and $+15°$ at a speed of 1.5 m/s. We averaged across strides the harvested power from the final 1 min of data and compared it to the corresponding literature mechanical power profiles. Level walking literature profiles were from Zelik and Kuo [15], while sloped walking profiles were from Lay *et al.* [18], [19].

Our controller was able to automatically and accurately modulate the timing and magnitude of energy harvesting for various steady state gaits (Figs. 8 and 9). For level walking, electrical power was produced during four phases of the gait cycle, all of which correspond to phases of negative mechanical knee joint power from the literature. The controller, which was calibrated only during level walking at 1.5 m/s, was also able to identify phases of negative joint power across a range of speeds and slopes (Figs. 8 and 9, respectively). For example, during decline walking the controller appropriately ceased harvesting at mid-stance (~35% gait cycle)—a phase in which harvesting occurred on the level. And within each phase, the controller automatically harvested increased levels of electrical power when greater power was available. This can be clearly seen during decline walking and at higher walking speeds.

We used three tasks to assess our controller's adaptability to sudden changes in gait. In the first task, we rapidly changed the treadmill speed every 20 s during a 2 min level walking trial. The speed alternated between 1.25 m/s and 1.6 m/s, with an acceleration of 0.1 $\mathrm{m/s^2}$. In the second task, again during a 2 min level walking trial, we held the treadmill speed constant at 1.5 m/s while the subject simulated stepping over a knee high object, such as a log, every 20th step with the left leg leading. The third task was of similar design to the second except every 20th step the subject lunged down on the left leg, as though bending so that their head could clear an overhead object.

The first task allowed us to assess our controller's responsiveness to rapid changes in gait. Within one step of a speed change, the power harvested immediately increased for increases in

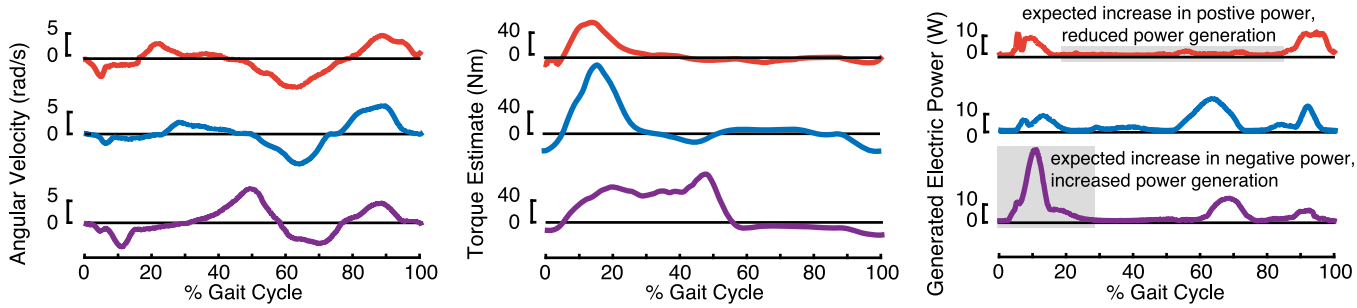

Fig. 10. Knee joint angular velocity (left column), torque estimate (middle column), and generated electric power (right column) for a high step (red; top row), normal step (blue; middle row), and downward lunge (purple; bottom row). Generated electric power is relatively low during mid gait cycle for the high step, when net knee joint mechanical power is expected to be positive, and is markedly increased during early gait cycle for the lunge, when net knee joint power is expected to be negative during lowering (regions indicated with grey shading). Walking speed was 1.5 m/s and data presented are from the left leg.

speed and decreased for decreases in speed ($+1.32 \pm 0.28$ W and -1.10 ± 0.17 W, respectively). The second task, where the subject performs a high step with their left leg, is a task for which we would expect minimal negative knee joint power. Indeed, we found that for these steps, the controller turned harvesting off throughout the 20%–80% of the gait cycle when we anticipate the leg is being lifted and accelerated (Fig. 10). In the third task, where the subject performs a lunge with their left leg, we would expect high negative knee joint power following heel strike as the subject flexes the knee to lower their body. Indeed, for these steps significant harvesting occurred in the 0%–30% phase of the gait cycle (Fig. 10).

V. Discussion

We have demonstrated that myoelectric control can be used to automatically adapt the timing and magnitude of electrical power generation for an energy harvesting exoskeleton. Our controller design engages power generation only when estimated knee joint mechanical power is negative. When engaged, the exoskeleton scales the resistive torque in proportion to estimated knee joint torque, thereby automatically scaling electrical power generation in proportion to the available negative mechanical power at the joint. Real-time estimates of knee joint torque and power are crucial to our controller's function and are produced using a simple model embedded within our controller that relies on muscle activity from knee joint flexors and extensors. We found that this model was able to predict knee joint dynamics across a range of timings and magnitudes. We demonstrated this using literature EMG data available for a range of walking speeds and found that estimates of knee joint torque and power well matched the corresponding literature profiles (torque R^2: 0.73–0.92; power R^2: 0.60–0.94). We also preformed preliminary experiments, which demonstrated that our myoelectric controller can be used to identify when the knee is generating negative mechanical power, and automatically adjust the magnitude of electrical power generation. It appeared to work well for a range of steady state walking speeds and inclines, as well as number of non-steady state walking conditions.

One limitation of this preliminary test of our controller is that we did not measure the knee joint torque and mechanical power for our particular subject. Instead, we relied on average literature profiles from able-bodied subjects. Our approach does have the benefit of more closely replicating exoskeleton use in a real-world setting, where capturing subject specific joint kinetics using inverse dynamics [34], [35], may be difficult and cumbersome. However, future work may still benefit from subject-specific joint kinetics during parameter identification, allowing model parameters to be optimized to a user's particular knee joint torque and power. This may be especially important for users that display atypical gait patterns, such as those with mobility impairments. We expect knee joint kinetics were quite similar to literature values for our able-bodied test subject, but even in our specific case, we may have benefited from subject-specific measures. For example, we found that the R muscle activity was not needed to predict literature values of knee joint power—for either leg an assigned gain of 0 produced near optimal power estimates. However, it is also possible that for this particular subject, the R muscle activity was responsible for a more pronounced atypical extensor torque that was not evident in the literature torque profile. Further testing is needed to determine when differences between individuals, and between limbs within an individual, necessitate user specific knee joint kinetics for parameter estimation. Another benefit of collecting subject-specific kinetics is that they could be used to further validate our controller's performance. EMG-derived estimates of knee joint torque and power from each trial would ideally be compared to the knee joint kinetics measured during that particular trial. This is because the interaction with the active exoskeleton may have caused actual knee joint kinetics to differ from generic literature profiles during steady state walking. Moreover, it would have provided us with joint kinetics for non-steady state walking conditions (conditions that are absent from the literature). Our use of literature values for parameter estimation and subsequent assessment of our controller performance demonstrate the potential usefulness of this type of control, which is likely to only improve with subject-specific measures.

Even with subject-specific joint torque and power profiles, the biomechanics and control of muscle action makes predicting optimal phases of harvesting difficult. As detailed by Li and Donelan, muscle co-contraction, bi-articular muscle architecture and elastic energy storage complicate the relationship between net joint power and true muscle power [13]. And for effective generative braking, a controller needs to assist muscles, not joints, in performing negative mechanical work.

There are a number of ways our myoelectric controller could be adapted to deal with these physiological complexities. For one, our controller could be used in combination with a state-machine that disengages or engages electrical power generation during phases of negative joint power that don't reflect true negative muscle power. For example, if it is determined that the negative joint work performed at the beginning of walking's stance phase is typically stored and returned to straighten the knee during the middle of stance, a modified controller may leverage measures of muscle activity to detect this event and turn off electrical power generation for this phase. With this hypothetical modification, our myoelectric controller would be used for the remainder of the walking cycle to modulate the timing and magnitude of power generation. Integrating our myoelectric controller within a state-machine certainly reduces the simplicity and generality of our controller, but the combination of the two may outperform either on their own.

Rather than modifying our controller to compensate for the complex relationship between joint and muscle power, it may instead be feasible to keep our controller exactly the same and control the action of the exoskeleton based on estimates of muscle torque and power, rather than joint torque and mechanical power. Much development has been directed towards musculoskeletal models that combine EMG with forward dynamic models to predict individual muscle velocities, forces and mechanical powers [20], [36], [37]. Future work may combine these models with our parameter identification procedure to find the optimal parameters for relating measured muscle activity to muscle torque and power. Using these muscle-optimized parameters with our myoelectric controller may improve the accuracy and efficiency of harvesting while preserving its generality and adaptability. It is also possible that these more complex musculoskeletal models are integrated within our controller in place of our simple model and used to estimate muscle force and power not just within the parameter identification procedure, but for all conditions. This would likely require a more extensive muscle set as well as real-time estimates of kinematics and kinetics from all lower limb joints. Given the success of our simplified controller, we suspect that any improvements in performance would not outweigh the drawbacks of added model and instrumentation complexity.

Our controller structure lends itself naturally to adaptive control. The controller initially has a small number of parameters, and we fix all but one of these using a parameter identification procedure. The remaining free parameter is the gain between estimated torque and applied torque (K)—it determines the relative contribution of the exoskeleton to the total joint torque and power. In our experiments, we evaluated a range of its values and found that there is a tradeoff between subject comfort (which is high at low values of K) and electrical power generation (which is high at high values of K). One use of this gain is to allow a user to manually adjust this single parameter to optimize their current needs—comfort or power. Rather than yield control to the user, the controller may instead employ adaptive control, adjusting this gain to meet some programmed objective. For example, the objective may be to maximize power generation while maintaining user comfort. As a user becomes more experienced with the exoskeleton and learns to take advantage of the assistance it provides, their muscle activity may reduce for a given value of K [30]. Sensing this, an adaptive controller could increase K to match the prior levels of muscle activity, increasing electrical power generation while attempting to maintain user comfort. Alternatively, the controller may regulate power generation by adapting K in order to keep a battery at some minimum charge. Whatever the programmed objective, it is convenient to have a single adjustable parameter.

While we have focused here on energy harvesting, our methods also apply to powered exoskeletons. For one, electrical motors in actuated exoskeletons may be used as generators to recover energy from the natural motion of walking. But more importantly, it is also possible that our EMG-derived estimates of joint torque and power be used to control exoskeletons that do not seek to harvest electrical power, but rather to assist movement. These exoskeletons need not be limited to those acting at the knee joint; our model of joint torque and power may work equally well using muscles that act about other joints. By translating the user's own neural signals, our controller design appears to adapt well to varied gaits and terrain.

ACKNOWLEDGMENT

The authors would like to thank the Locomotion Lab for their helpful comments and suggestions, as well as Bionic Power Inc., for providing the necessary exoskeleton hardware.

REFERENCES

[1] B. Dellon and Y. R. A. M. I. Matsuoka, "Prosthetics, exoskeletons, rehabilitation [Grand Challenges of Robotics]," *IEEE Robot. Automat. Mag.*, vol. 14, no. 1, pp. 30–34, Mar. 2007.

[2] A. M. Dollar and H. Herr, "Lower extremity exoskeletons and active orthoses: Challenges and state-of-the-art," *IEEE Trans. Robot.*, vol. 24, no. 1, pp. 144–158, Feb. 2008.

[3] R. Jiménez-Fabián and O. Verlinden, "Review of control algorithms for robotic ankle systems in lower-limb orthoses, prostheses, exoskeletons," *Med. Eng. Phys.*, vol. 34, no. 4, pp. 397–408, May 2012.

[4] J. M. Donelan *et al.*, "Biomechanical energy harvesting: Generating electricity during walking with minimal user effort," *Science*, vol. 319, no. 5864, pp. 807–810, Feb. 2008.

[5] Q. Li *et al.*, "Biomechanical energy harvesting: Apparatus and method," in *Proc. IEEE Int. Conf. Robot. Automat.*, 2008, pp. 3672–3677.

[6] J. M. Donelan, R. Kram, and A. D. Kuo, "Mechanical work for step-to-step transitions is a major determinant of the metabolic cost of human walking," *J. Exp. Biol.*, vol. 205, no. 23, pp. 3717–3727, Dec. 2002.

[7] P. Malcolm, W. Derave, S. Galle, and D. De Clercq, "A simple exoskeleton that assists plantarflexion can reduce the metabolic cost of human walking," *PLoS ONE*, vol. 8, no. 2, p. e56137-7, Feb. 2013.

[8] C. H. Soo and J. M. Donelan, "Coordination of push-off and collision determine the mechanical work of step-to-step transitions when isolated from human walking," *Gait Posture*, pp. 1–6, Oct. 2011.

[9] S. H. Collins and R. W. Jackson, "Inducing self-selected human engagement in robotic locomotion training," in *Proc. IEEE Int. Conf. Rehabil. Robot.*, 2013, pp. 1–6.

[10] A. D. Kuo, J. M. Donelan, and A. Ruina, "Energetic consequences of walking like an inverted pendulum: Step-to-step transitions," *Exercise Sport Sci. Rev.*, vol. 33, no. 2, pp. 88–97, Apr. 2005.

[11] J. M. Donelan, R. Kram, and A. D. Kuo, "Simultaneous positive and negative external mechanical work in human walking," *J. Biomech.*, vol. 35, no. 1, pp. 117–124, Jan. 2002.

[12] J. S. Gottschall and R. Kram, "Energy cost and muscular activity required for propulsion during walking," *J. Appl. Physiol.*, vol. 94, no. 5, pp. 1766–1772, May 2003.

[13] Q. Li, V. Naing, and M. J. Donelan, "Development of a biomechanical energy harvester," *J. Neuroeng. Rehabil.*, vol. 6, no. 1, p. 22, 2009.
[14] Z. Rubinshtein, M. M. Peretz, and R. Riemer, "Biomechanical energy harvesting system with optimal cost-of-harvesting tracking algorithm," in *Proc. 29th Annu. IEEE Appl. Power Electron. Conf. Expo.*, 2014, pp. 3105–3109.
[15] K. E. Zelik and A. D. Kuo, "Human walking isn't all hard work: Evidence of soft tissue contributions to energy dissipation and return," *J. Exp Biol.*, vol. 213, no. 24, pp. 4257–4264, Nov. 2010.
[16] J. J. Eng and D. A. Winter, "Kinetic analysis of the lower limbs during walking: What information can be gained from a three-dimensional model?," *J. Biomech.*, vol. 28, no. 6, pp. 753–758, Jun. 1995.
[17] C. E. Mullins and D. L. Hepler, "Methods and apparatus for control of biomechanical energy harvesting," U.S. Patent 20 140 353 970, 2014.
[18] A. N. Lay, C. J. Hass, and R. J. Gregor, "The effects of sloped surfaces on locomotion: A kinematic and kinetic analysis," *J. Biomechan.*, vol. 39, no. 9, pp. 1621–1628, Jan. 2006.
[19] A. N. Lay, C. J. Hass, T. Richard Nichols, and R. J. Gregor, "The effects of sloped surfaces on locomotion: An electromyographic analysis," *J. Biomech.*, vol. 40, no. 6, pp. 1276–1285, 2007.
[20] D. G. Lloyd and T. F. Besier, "An EMG-driven musculoskeletal model to estimate muscle forces and knee joint moments *in vivo*," *J. Biomech.*, vol. 93, no. 6, pp. 765–776, Jun. 2003.
[21] T. S. Buchanan, D. G. Lloyd, K. Manal, and T. F. Besier, "Neuromusculoskeletal modeling: Estimation of muscle forces and joint moments and movements from measurements of neural command," *J. Appl. Biomech.*, vol. 20, no. 4, pp. 367–395, Nov. 2004.
[22] A. L. Hof and J. Van den Berg, "EMG to force processing I: An electrical analogue of the Hill muscle model," *J. Biomech.*, vol. 14, no. 11, pp. 747–758, 1981.
[23] P. R. Cavanagh and P. V. Komi, "Electromechanical delay in human skeletal muscle under concentric and eccentric contractions," *Eur. J. Appl. Physiol. Occup. Physiol.*, vol. 42, no. 3, pp. 159–163, Nov. 1979.
[24] R. W. Norman and P. V. Komi, "Electromechanical delay in skeletal muscle under normal movement conditions," *Acta Physiol. Scand.*, vol. 106, no. 3, pp. 241–248, Jul. 1979.
[25] A. Fougner, O. Stavdahl, P. J. Kyberd, Y. G. Losier, and P. A. Parker, "Control of upper limb prostheses: Terminology and proportional myoelectric control—A review," *IEEE Trans. Neural Syst. Rehabil. Eng.*, vol. 20, no. 5, pp. 663–677, Sep. 2012.
[26] M. Asghari Oskoei and H. Hu, "Myoelectric control systems—A survey," *Biomed. Signal Proces*, vol. 2, no. 4, pp. 275–294, Oct. 2007.
[27] P. Parker, K. Englehart, and B. Hudgins, "Myoelectric signal processing for control of powered limb prostheses," *J. Electromyogra Kines.*, vol. 16, no. 6, pp. 541–548, Dec. 2006.
[28] S. K. Au, P. Bonato, and H. Herr, "An EMG-position controlled system for an active ankle-foot prosthesis: An initial experimental study," in *Proc. 9th Int. Conf. Rehabil. Robot.*, 2005, pp. 375–379.
[29] S. Au, M. Berniker, and H. Herr, "Powered ankle-foot prosthesis to assist level-ground and stair-descent gaits," *Neural Netw.*, vol. 21, no. 4, pp. 654–666, May 2008.
[30] D. P. Ferris, K. E. Gordon, G. S. Sawicki, and A. Peethambaran, "An improved powered ankle-foot orthosis using proportional myoelectric control," *Gait Posture*, vol. 23, no. 4, pp. 425–428, Jun. 2006.
[31] D. P. Ferris, J. M. Czerniecki, and B. Hannaford, "An ankle-foot orthosis powered by artificial pneumatic muscles," *J. Appl. Biomech.*, vol. 21, no. 2, pp. 189–197, May 2005.
[32] S. Lee and Y. Sankai, "Power assist control for walking aid with HAL-3 based on EMG and impedance adjustment around knee joint," in *Proc. IEEE Int. Conf. Intell. Robots Syst.*, 2002, vol. 2, pp. 1499–1504.
[33] A. L. Hof, H. Elzinga, W. Grimmius, and J. P. K. Halbertsma, "Speed dependence of averaged EMG profiles in walking," *Gait Posture*, vol. 16, no. 1, pp. 78–86, Aug. 2002.
[34] M. P. Kadaba, H. K. Ramakrishnan, and M. E. Wootten, "Measurement of lower extremity kinematics during level walking," *J. Orthop. Res.*, vol. 8, no. 3, pp. 383–392, May 1990.
[35] R. B. Davis, S. Ounpuu, D. Tyburski, and J. R. Gage, "A gait analysis data collection and reduction technique," *Hum Mov Sci*, vol. 10, no. 5, pp. 575–587, 1991.
[36] M. G. Hoy, F. E. Zajac, and M. E. Gordon, "A musculoskeletal model of the human lower extremity: The effect of muscle, tendon, moment arm on the moment-angle relationship of musculotendon actuators at the hip, knee, ankle," *J. Biomech.*, vol. 23, no. 2, pp. 157–169, 1990.
[37] S. L. Delp *et al.*, "OpenSim: Open-source software to create and analyze dynamic simulations of movement," *IEEE Trans. Biomed. Eng.*, vol. 54, no. 11, pp. 1940–1950, Oct. 2007.

Jessica C. Selinger received the B.S. degree in life sciences and the M.S. degree in biomechanics from Queen's University, Kingston, ON, Canada in 2007 and 2009, respectively. She is currently a Ph.D. degree candidate in the Department of Biomedical Physiology and Kinesiology, Simon Fraser University, Burnaby, BC, Canada.

Her research interests include the biomechanics, energetics, and neurophysiology of legged locomotion, as well as human–machine interactions and the design and control of exoskeletons and orthoses.

J. Maxwell Donelan received the B.S. degree in kinesiology from McMaster University, Hamilton ON, Canada, in 1995, the M.Sc. degree in human biodynamics, and the Ph.D. degree in integrative biology from the University of California at Berkeley, Berkeley, CA, USA, in 1997 and 2001, respectively.

He is currently a Professor in the Department of Biomedical Physiology and Kinesiology, Simon Fraser University, Burnaby, BC, Canada. His research interests are focused on understanding fundamental neuromechanical principles of movement in humans and other animals, as well as the application of these principles, including to energy harvesting technologies.